DIFFRACTIVE SCATTERING AT HERA

PAUL NEWMAN [a] for the H1 and ZEUS Collaborations
School of Physics and Astronomy, University of Birmingham,
Birmingham B15 2TT, England

Recent measurements of diffractive deep-inelastic scattering at HERA are described. The effective pomeron describing the energy dependence of the $\gamma^\star p$ interaction has intercept $\alpha_{\mathbb{P}}(0)$ larger than that governing soft hadronic interactions. When a partonic structure is ascribed to the pomeron, QCD analysis of the diffractive cross section reveals that $80-90\%$ of the exchanged momentum is carried by a 'hard' gluon distribution in the kinematic region $4.5 < Q^2 < 75$ GeV^2. This result is confirmed in studies of the hadronic final state.

1 Introduction

The concept of a pomeron ($\mathbb{P}$) trajectory, possessing vacuum quantum numbers and mediating diffractive scattering, has proved remarkably successful in formulating a Regge description of high energy hadronic cross sections.[1] There has been considerable recent interest in understanding the underlying dynamics of diffractive interactions in terms of quantum chromodynamics (QCD). At the HERA ep collider, the partonic nature of diffractive interactions has been studied by the introduction of a variety of hard scales.

The generic diffractive process $ep \rightarrow eXY$ at HERA is illustrated in figure 1a. The two systems X and Y comprising the hadronic final state are clearly separated in rapidity, Y being the system closest to the outgoing proton direction. With k and P denoting the 4-vectors of the incoming electron and proton respectively and q the 4-vector of the photon, the standard kinematic variables $Q^2 \equiv -q^2$, $y \equiv (q \cdot P)/(k \cdot P)$ and $W^2 \equiv (q+P)^2$ are defined. With p_X and p_Y representing the 4-vectors of the two distinct components of the hadronic final state, the data are also discussed in terms of

$$M_X^2 \equiv p_X^2 \qquad M_Y^2 \equiv p_Y^2 \qquad t \equiv (P - p_Y)^2 \qquad x_{\mathbb{P}} \equiv \frac{q \cdot (P - p_Y)}{q \cdot P} \qquad \beta \equiv \frac{Q^2}{2q \cdot (P - p_Y)} \; , \quad (1)$$

[a] Supported by the UK Particle Physics and Astronomy Research Council (PPARC).

where t is the squared four-momentum transferred between the photon and the proton, $x_{I\!P}$ is the fraction of the proton beam momentum transferred to the system X and β may be considered as the fraction of the exchanged 4-momentum that is carried by the quark coupling to the photon.

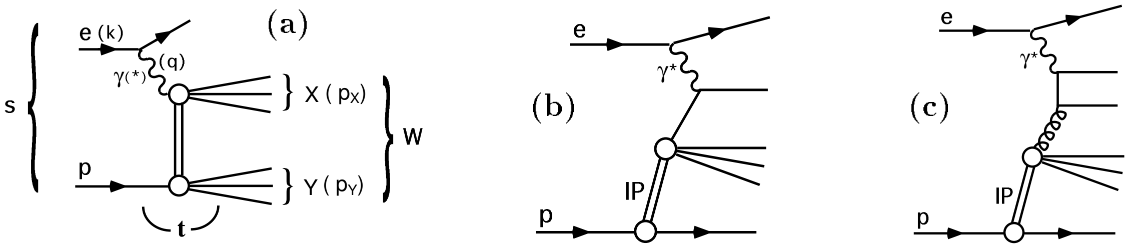

Figure 1: (a) Illustration of the generic process, $ep \to eXY$. (b, c) Lowest order hard processes by which a quark or a gluon from the pomeron parton distributions can couple to a photon. (b) The 'Quark Parton Model' process, initiated by a quark from the pomeron. (c) The 'Boson-Gluon Fusion' process, initiated by a gluon from the pomeron.

The discussion here is restricted to the kinematic region in which $|t|$ is small and a large value of Q^2 sets a hard scale. If the pomeron can be considered as a partonic system,[2] the process can be considered as deep-inelastic scattering (DIS) from a distinct set of pomeron parton distributions. If the diffractive interaction is modelled in terms of the exchange of two gluons in a net colour-singlet configuration from the proton parton distributions,[3] the data are sensitive to the partonic fluctuations into which the virtual photon can be excited.

2 Semi-Inclusive Cross Sections

Semi-inclusive measurements have been made by both H1 and ZEUS of the DIS interaction $ep \to eXY$. The mass of the system Y is constrained to be as small as possible, such that the data samples are dominated by the single dissociation process where Y is a proton. The analyses are restricted to small $x_{I\!P}$, where diffraction is expected to dominate.

Three different experimental techniques have been used for the selection of data samples. In the first, purpose-designed forward proton spectrometers (FPSs) are exploited to detect and measure final state protons. Figure 2a shows the t distribution as measured using the ZEUS FPS.[4] The data are well described by a simple parameterisation of the form $\mathrm{d}\sigma/\mathrm{d}t \propto e^{bt}$, with $b = 7.2 \pm 1.1$ (stat.) $^{+0.7}_{-0.9}$ (syst.) GeV^{-2}, revealing a highly peripheral scattering characteristic of a diffractive process.

Both collaborations have made measurements using a second selection method, based on the presence of a large rapidity gap adjacent to the final state proton or its excitation. The system X is measured in the central parts of the detectors. This approach considerably enhances statistics and the accessible kinematic range as compared with the FPS method, but it is not possible to measure t or to constrain the system Y to be a single proton. The H1 measurements are integrated over the kinematic range $M_Y < 1.6$ GeV and $|t| < 1.0$ GeV^2 and are presented in terms of a three dimensional structure function $F_2^{D(3)}(\beta, Q^2, x_{I\!P})$, defined in close analogy to the inclusive proton structure function as

$$\frac{\mathrm{d}\sigma^{ep\to eXY}}{\mathrm{d}\beta\ \mathrm{d}Q^2\ \mathrm{d}x_{I\!P}} = \frac{4\pi\alpha^2}{\beta Q^4}\ (1 - y + \frac{y^2}{2})\ F_2^{D(3)}(\beta, Q^2, x_{I\!P})\ . \tag{2}$$

Measurements have been made at 73 points in the β and Q^2 kinematic plane,[5] two of which are shown in figure 2b. A clear variation in the $x_{I\!P}$ dependence of $F_2^{D(3)}$ is observed with β. This has been interpreted in a model based on Regge phenomenology in terms of the presence of both a diffractive ($I\!P$) and a sub-leading ($I\!R$) exchange in the kinematic region studied. It is assumed

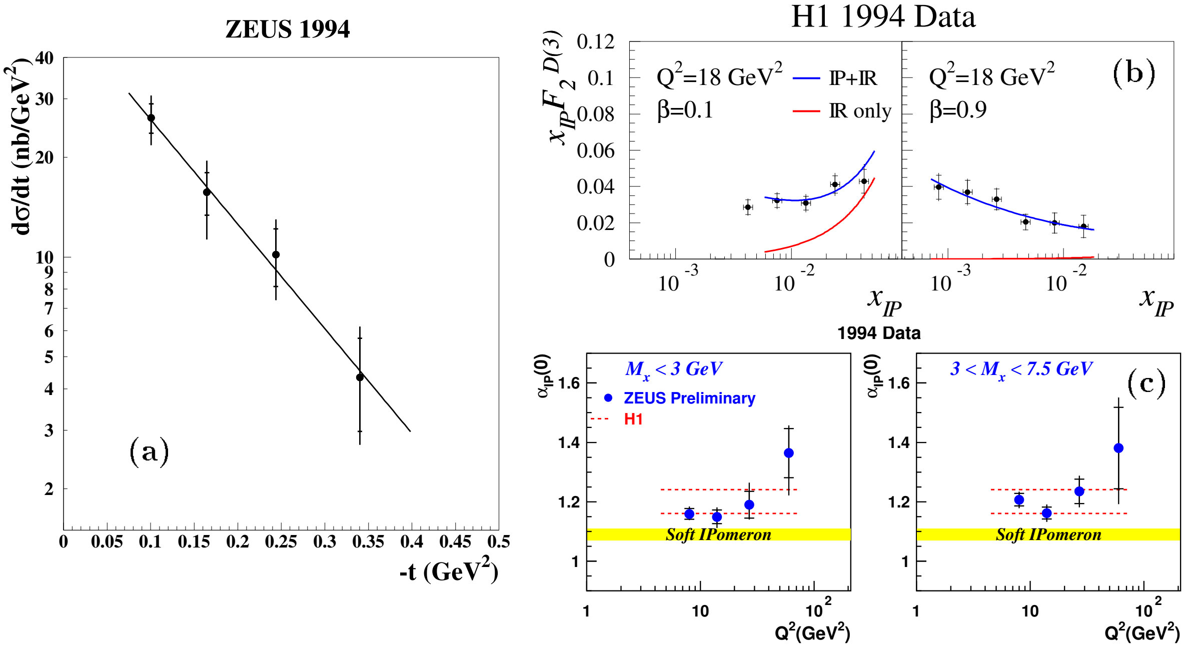

Figure 2: (a) Differential t-distribution in the kinematic region $5 < Q^2 < 20$ GeV^2, $0.015 < \beta < 0.5$ and $x_{\mathbb{P}} < 0.03$, obtained using the ZEUS FPS. (b) Example H1 measurements of $x_{\mathbb{P}} \cdot F_2^{D(3)}$, together with the results of a fit to the parameterisation of equations 3 and 4. (c) Comparison of H1 and ZEUS extractions of $\alpha_{\mathbb{P}}(0)$, compared to the value expected for the 'soft' pomeron that governs hadronic interactions in the absence of hard scales.

that for each exchange, the (β, Q^2) dependence factorises from the $x_{\mathbb{P}}$ dependence according to

$$F_2^{D(3)} \;=\; f_{\mathbb{P}/\mathrm{p}}(x_{\mathbb{P}})\; F_2^{\mathbb{P}}(\beta, Q^2) \;+\; f_{\mathbb{R}/\mathrm{p}}(x_{\mathbb{P}})\; F_2^{\mathbb{R}}(\beta, Q^2) \tag{3}$$

where $F_2^i(\beta, Q^2)$ is proportional to the structure function for the exchanged object i and

$$f_{i/\mathrm{p}}(x_{\mathbb{P}}) = \int_{-1\mathrm{GeV}^2}^{t_{min}(x_{\mathbb{P}})} \left(\frac{1}{x_{\mathbb{P}}}\right)^{2\alpha_i(t)-1} e^{B_i t}\, \mathrm{d}t \tag{4}$$

is a parameterisation of the flux factor for the exchange i from the proton. $\alpha_i(t) = \alpha_i(0) + \alpha_i' t$ is the trajectory for the exchange i and B_i is the slope parameter for that exchange at $x_{\mathbb{P}} = 0$. Fits are performed in which $\alpha_{\mathbb{P}}(0)$, $\alpha_{\mathbb{R}}(0)$ and the values of $F_2^{\mathbb{P}}$ and $F_2^{\mathbb{R}}$ at each (β, Q^2) point are free parameters and the remaining parameters are taken from soft diffractive data. The sub-leading trajectory contributes most strongly at large $x_{\mathbb{P}}$ due to the smaller value of $\alpha_{\mathbb{R}}(0)$ than $\alpha_{\mathbb{P}}(0)$ and at small β due to the differences in the shapes of $F_2^{\mathbb{P}}$ and $F_2^{\mathbb{R}}$.

The third selection procedure, employed by ZEUS,[6] is based on the fact that different exchanges are expected to give rise to different M_X distributions. In bins of W and Q^2, the reconstructed M_X distribution is subjected to a fit of the form

$$\mathrm{d}\mathcal{N}/\mathrm{d}\ln M_X^2 = D_1 + \frac{D_2}{M_X^2} + c\, e^{b \ln M_X^2}\ , \tag{5}$$

with D_1, D_2, b and c as free parameters. The operationally defined diffractive contribution D_1 is acceptance corrected to give cross sections in two intervals of M_X for the process $ep \to eXY$ with $M_Y \lesssim 4$ GeV. The t averaged value of the pomeron intercept, $\overline{\alpha_{\mathbb{P}}}$, is then extracted at fixed Q^2 by fitting to the Regge motivated form

$$\frac{\mathrm{d}\sigma_D^{ep\to eXY}}{\mathrm{d}M_X}(M_X, W, Q^2) \propto \left(W^2\right)^{2\,\overline{\alpha_{\mathbb{P}}}-2}\ . \tag{6}$$

The results for $\alpha_{I\!P}(0)$ are shown in figure 2c after applying the correction $\alpha_{I\!P}(0) = \overline{\alpha_{I\!P}} + 0.03$. They are compared with the H1 value of $\alpha_{I\!P}(0) = 1.203 \pm 0.020$ (stat.)± 0.013 (syst.) $^{+0.030}_{-0.035}$(model), obtained from fits using equations 3 and 4. The two experiments are found to be in reasonable agreement, with the pomeron intercept significantly larger than the values $\alpha_{I\!P} \sim 1.1$ obtained from soft diffractive processes.[7]

The β and Q^2 dependences of $F_2^{D(3)}$ are presented at fixed small values of $x_{I\!P}$ in figures 3a and 3b respectively. Scaling violations in the Q^2 dependence with positive $\partial F_2^D/\partial \log Q^2$ persist to large values of β. The β dependence displays a relatively flat structure, with significant contributions at large fractional momenta.

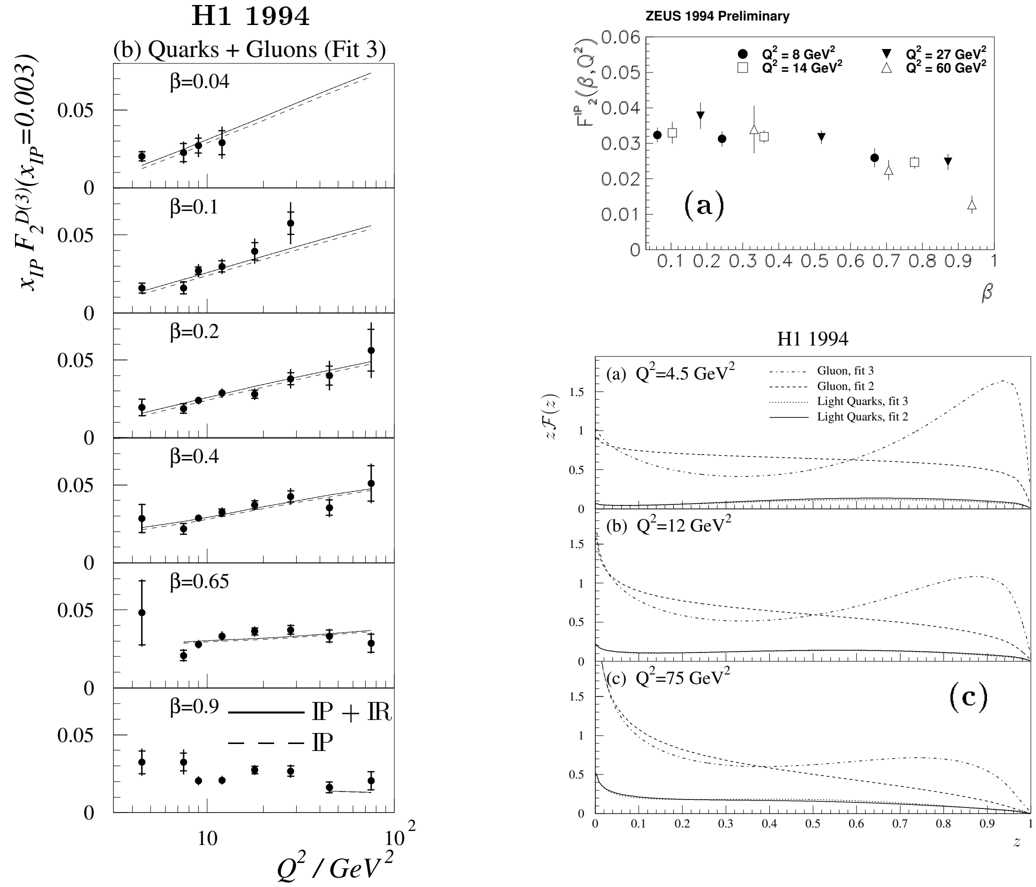

Figure 3: (a) ZEUS measurement of the β dependence of $F_2^{D(3)}$ at various values of Q^2 and $x_{I\!P} = 0.0042$. (b) H1 measurement of the Q^2 dependence of $F_2^{D(3)}$ at various β values and $x_{I\!P} = 0.003$. The results of the DGLAP fit described in section 2 in which both quarks and gluons contribute at the starting scale for evolution are also shown. (c) The pomeron parton distributions extracted in two fits in which both singlet-quarks and gluons contribute at the starting scale for DGLAP evolution.

In factorisable partonic pomeron models,[2] these features indicate the need for a significant 'hard' (large $z \equiv x_{g/I\!P}$) gluon contribution to the pomeron structure. The H1 fits to the $x_{I\!P}$ dependence have been extended to describe the β and Q^2 dependence with a QCD analysis in which singlet quark and gluon distributions are ascribed to the pomeron, evolving according to the DGLAP equations.[5] The results from the best fit of this type are shown in figure 3b. The parton distributions obtained are shown in figure 3c. In these fits, more than 80 % of the pomeron momentum is carried by gluons throughout the Q^2 range studied. The β and Q^2 dependence of F_2^D has also been interpreted in a model based on the exchange of 2 gluons from the proton parton distributions. A recent parameterisation[8] indicates the need for both $q\bar{q}$ and $q\bar{q}g$ photon fluctuations, with significant higher twist contributions at large β and low Q^2.

3 Analysis of the Final State System X

Many final state observables are sensitive to the partonic structure of the diffractive interaction. First publications on HERA data have appeared on event shapes,[9,10] energy flow and charged particle spectra,[11,12] charged particle multiplicities and their correlations[13] and dijet production rates.[14,15] The natural frame in which to study the final state is the rest frame of the system X ($\gamma^\star I\!P$ centre of mass frame), the natural direction in that frame being the $\gamma^\star I\!P$ collision axis.

In models with a factorisable partonic pomeron, the lowest order hard process by which a quark couples to a photon is the 'quark-parton model' (QPM) diagram (figure 1b). The lowest order process by which a gluon can couple to a photon is boson-gluon fusion (BGF) (figure 1c). These processes lead to rather different characteristics of the final state system X. The QPM interaction yields final states consisting of a colour triplet and an anti-triplet, which are in general highly aligned with the $\gamma^\star I\!P$ collision axis. Few high transverse momentum (p_T) particles are expected. By contrast, the virtual quark propagator in the BGF process can give rise to final states that are not aligned with the $\gamma^\star I\!P$ axis, with more copious high p_T particle production and octet-octet correlations.

Example results from final state analyses are shown in figures 4 and 5. Figure 4a shows the p_T^2 distribution of charged particles comprising the system X,[11] compared with inclusive μp data at a value of W that is close to M_X in the diffractive data, corresponding to a region in which proton structure is quark dominated. The diffractive data exhibit a significantly harder p_T^2 distribution than the inclusive DIS data, indicating that contributions from $q\bar{q}g$ final states are important. This is confirmed by comparisons with the RAPGAP Monte Carlo model implementation of the H1 QCD fits to $F_2^{D(3)}$, with a good description of the data occurring only when the pomeron parton distributions are dominated by 'hard' gluons.

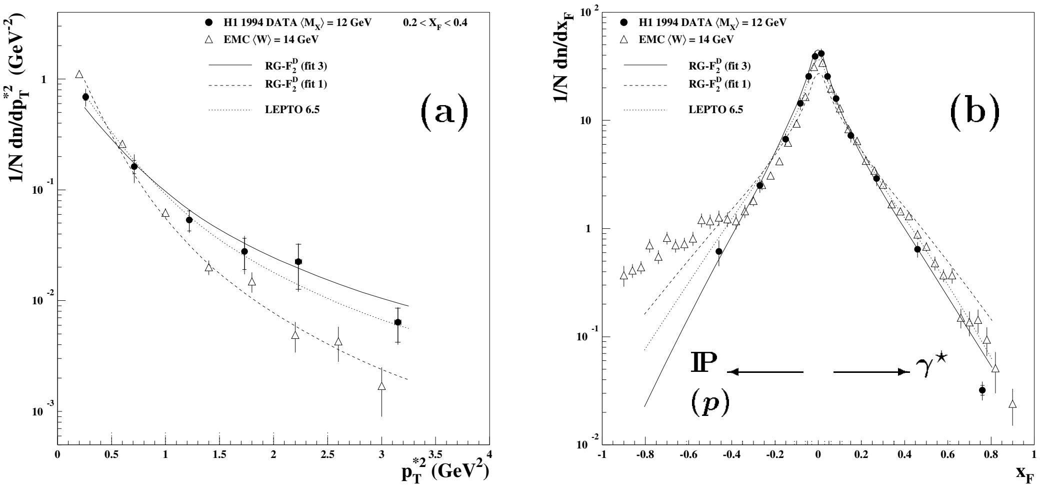

Figure 4: Charged particle distributions for the final state system X compared to inclusive μp data and to the RAPGAP model of a partonic pomeron with gluon (F_2^D fit 3) and quark (F_2^D fit 1) dominated structure. (a) p_T^2 distribution. (b) x_F distribution.

Figure 4b shows the charged particle distribution in x_F,[11] compared to the same μp data.[b] The x_F distribution is approximately symmetric in the diffractive case, with no evidence for the extended remnant in the target direction that is characteristic of lepton-nucleon DIS. Again, the data are well described by the RAPGAP model with gluon dominated pomeron structure.

Figure 5a shows the event thrust[10] as a function of $1/M_X$ compared to e^+e^- data at centre of mass energy equal to M_X. The leading hard process in the e^+e^- data is the production of a simple $q\bar{q}$ pair. The fact that the H1 data lie significantly lower in thrust than the e^+e^- data at

[b] The Feynman variable is defined here as $x_F = 2p_L^\star/M_X$, where p_L is the charged particle longitudinal momentum.

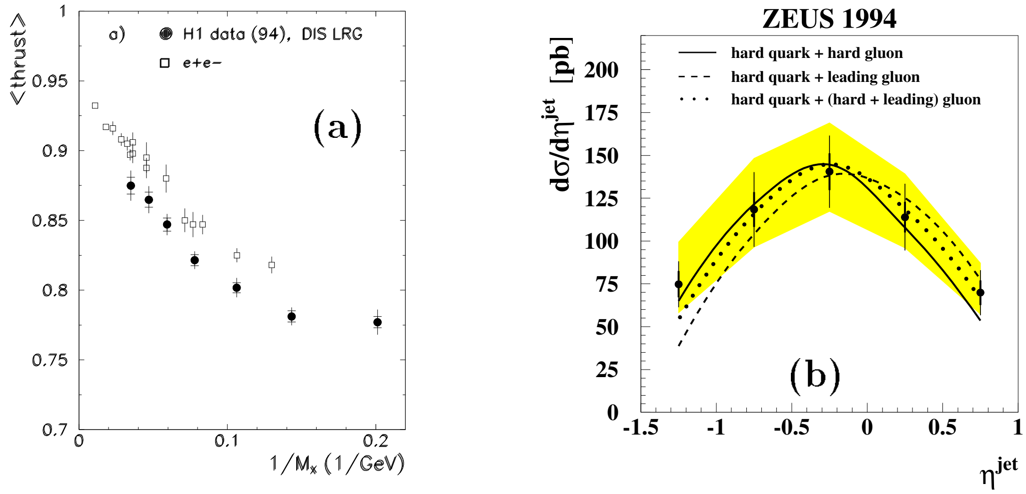

Figure 5: (a) Mean thrust distribution of H1 diffractive data compared to a compilation of e^+e^- data at centre of mass energies equivalent to M_X. (b) Laboratory pseudorapidity distribution of ZEUS data on diffractive dijet photoproduction ($E_t^{\rm jet} > 6$ GeV). The results of combined DGLAP fits to these data and F_2^D are shown in which the pomeron structure is dominated by 'hard' gluon distributions.

all M_X is again indicative of the presence of more complex final states such as $q\bar{q}g$, as expected for a gluon dominated exchange.

Figure 5b shows a measurement of the pseudorapidity distribution of diffractively produced dijets in photoproduction.[15] These data are predominantly sensitive to the $\mathcal{O}(\alpha_{\rm em}\alpha_s)$ processes BGF and QCD-Compton (figure 1b with an additional gluon emission). A combined leading order DGLAP fit is performed to the dijet data at a scale E_t and a measurement[16] of $F_2^{D(3)}$. The relatively high rate of dijet production cannot be reproduced with a quark dominated pomeron. Good fits are obtained with a variety of parameterisations of the pomeron structure that feature a dominant 'hard' gluon distribution.

References

1. K. Goulianos, *Phys. Rep.* **101**, 169 (1983).
2. G. Ingelman, P. E. Schlein, *Phys. Lett.* B **152**, 256 (1985).
3. F. Low, *Phys. Rev.* D **12**, 163 (1975).
   S. Nussinov, *Phys. Rev. Lett.* **34**, 1286 (1975).
4. ZEUS Collab., J. Breitweg et al., *Eur. Phys. J.* C **1**, 81 (1998).
5. H1 Collab., C. Adloff et al., *Z. Phys.* C **76**, 613 (1997).
   H1 Collab., paper 377 at Int. Europhys. Conf. on HEP, Jerusalem, August 1997.
6. ZEUS Collab., paper 638 at Int. Europhys. Conf. on HEP, Jerusalem, August 1997.
7. A. Donnachie, P. Landshoff, *Phys. Lett.* B **296**, 227 (1992).
   H1 Collab., C. Adloff et al., *Z. Phys.* C **74**, 221 (1997).
8. J. Bartels et al., , DESY 98-034.
9. ZEUS Collab., J. Breitweg et al., *Phys. Lett.* B **421**, 368 (1998).
10. H1 Collab., C. Adloff et al., *Eur. Phys. J.* C **1**, 495 (1998).
11. H1 Collab., C. Adloff et al., DESY 98-029, submitted to *Phys. Lett.* B.
12. ZEUS Collab., paper 660 at Int. Europhys. Conf. on HEP, Jerusalem, August 1997.
13. H1 Collab., C. Adloff et al., DESY 98-044, submitted to *Eur. Phys. J.*
14. P. Marage, H1 Collab., Procedings of the 5th International Workshop on DIS and QCD, Chicago USA, April 1997.
15. ZEUS Collab., J. Breitweg et al., DESY 98-045, submitted to *Eur. Phys. J.*
16. ZEUS Collab., M. Derrick et al., *Z. Phys.* C **68**, 569 (1995).